Journal of Physics: Conference Series

**PAPER** • **OPEN ACCESS**

# Liquid holdup measurement for gas-liquid stratified flows by means of resistive probes and image processing

To cite this article: I M Carraretto *et al* 2022 *J. Phys.: Conf. Ser.* **2177** 012034

View the article online for updates and enhancements.

You may also like

- Liquid Holdup Measurement in Crude Oil Transportation Using Capacitance Sensors and Electrical Capacitance Tomography: Concept Review
Emmanuel E. Okoro, Josephs E. Rachael, Samuel E. Sanni et al.
- Direct estimation of gas holdup in gas–liquid bubble column reactors using ultrasonic transmission tomography and artificial neural processing
Jingyi Hu, Nan Li, Lina Wang et al.
- A novel online technique for water conductivity detection of vertical upward oil–gas–water pipe flow using conductance method
Da-Yang Wang, Ning-De Jin, Lu-Sheng Zhai et al.


This content was downloaded from IP address 131.175.28.235 on 09/05/2022 at 15:38

# Liquid holdup measurement for gas-liquid stratified flows by means of resistive probes and image processing

**I M Carraretto[1], L P M Colombo[1] and M Guilizzoni[1]**

[1]Politecnico di Milano, Dept. of Energy, via Lambruschini 4, 20156 Milan, Italy

igormatteo.carraretto@polimi.it

**Abstract**. Flow patterns exert a fundamental influence on the behaviour of multiphase flows, and they must be brought into play when dealing with their modelling. This is usually done by means of summarizing quantities as the phase holdups and the interfacial area concentration. Many techniques have been designed during the years to measure them, among which the use of probes relying on electrical resistance is one of the simplest and less expensive. While having these points of strength, resistive probes are intrusive devices. This work is therefore devoted to a comparison between liquid height (and derived quantities) measurements – for stratified and stratified-wavy air-water flows – performed using a conventional resistive probe and by means of an image-based technique. Validation of the latter was performed using computer-generated flow images. Then, an experimental campaign was carried out for flows with liquid superficial velocities in the range 0.03 ÷ 0.06 m/s and gas superficial velocities in the range 0.77 ÷ 2.31 m/s. Results showed that the two methods give answers within very few percent of difference, which is more than satisfactory in this field. The results are also in good agreement with some of the most credited literature models and correlations.

## 1. Introduction

In the study of multiphase flows, the distribution of the phases within the duct plays a fundamental role and it is usually taken into account in the models by means of quantities as the phase density function, the phase holdups and the interfacial area concentration [1]. Sampling of such quantities is far from being an easy task and many techniques have been designed during the years, ranging from very complex and expensive ones (e.g., gamma-ray attenuation, high speed X-ray tomography, magnetic resonance imaging and wire mesh sensors; reference to some fundamental papers about these techniques can be found in [2]) to much simpler devices as the different types of optical and electrical impedance probes which have been revised during the years ([3]–[8]).

In fact, in many multiphase flows, the phases have significantly different refraction indices and electrical impedances, and local, section- or volume- averaged measurements based on these quantities can reveal information about their spatial and temporal distribution within the flow. With a suitable selection of the probe geometry and appropriate calibration, such probes have been used to measure a variety of multiphase flow quantities, including film thickness in annular flows and liquid height in stratified flows (e.g., measuring the liquid layer depth by detection of the interface, thanks to a resistive probe in flush-wire configuration, as described in [8]). In fact, they can generate a practically "Boolean" voltage signal when the probe tip switches from a phase to the other, crossing the interface.

However, they are an intrusive method, i.e., it is needed to have holes on the ducts under analysis and the flow may be affected – even if minimally –by the presence of the probe. Hence image-based

Content from this work may be used under the terms of the Creative Commons Attribution 3.0 licence. Any further distribution of this work must maintain attribution to the author(s) and the title of the work, journal citation and DOI.
Published under licence by IOP Publishing Ltd

methods were developed, based on the processing of external views of the flow. (typically, from the side, e.g., [9]). In this work, a technique suitable for stratified flows is presented and its results are compared with those from resistive probes.

## 2. Experimental set-up and operating conditions

The experimental activity was carried out in the laboratory of Multiphase Thermal-Fluid Dynamics at the Department of Energy, Politecnico di Milano.

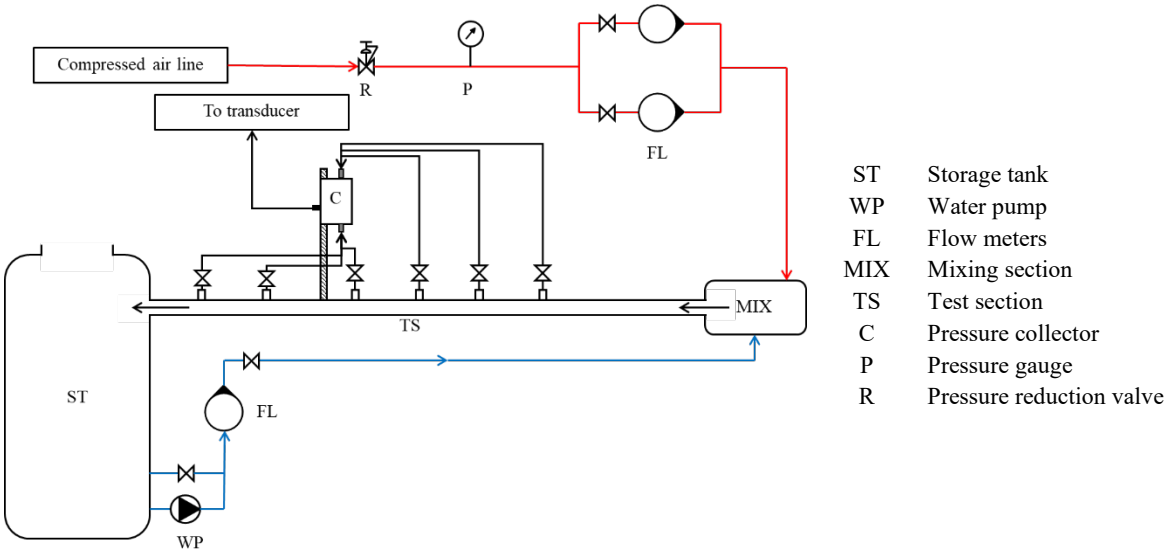


**Figure 1.** Layout of the experimental setup

The liquid is supplied from the bottom of a 4.0 $m^3$ storage tank by means of a CALPEDA centrifugal pump (volume flow rate = 0.12 ÷ 0.75 $m^3/h$; head = 6.5 ÷ 20 m). The liquid flow rate is measured by a float-type flow meter (whose characteristics are reported in Table 1) and set through a bypass valve upstream of the flow meter. Air flow rate is provided by the Department compressed air line at 0.8 MPa and measured by a float-type flow meter, the reading of which is suitably corrected to account for pressure and temperature deviation from standard conditions; the working point is set both through a pressure reducing valve and the flow meter valve. The liquid and the gas are injected into a mixing section, subsequently the two-phase flow enters the test section, that is made of transparent PMMA ducts having 60 mm inner diameter and 5 mm thickness. More details about the setup, reported in Figure 1, can be found in [10] and in [11].

**Table 1.** Flow meters characteristics

| Name | Fluid | Full Scale (FS) | Error | $T_c$ [° C] | $P_c$ [Pa] |
|---|---|---|---|---|---|
| ASAMETRO P13-2800 | Water | 0.1 ÷ 1 $m^3/h$ | ± 3 % FS | 20 | - |
| ASAMETRO N5-2008 | Air | 2.5 ÷ 23.5 $m^3/h$ | ± 2.5 % FS | 20 | 101 325 |

The superficial velocities of the phases for the flow conditions investigated in this work were $J_L$ = 0.03 ÷ 0.06 m/s for the liquid and $J_G$ = 0.77 ÷ 2.31 m/s for the gas. Within these ranges, the flow was perfectly stratified or stratified with small-amplitude waves. Therefore, the liquid holdup, $\varepsilon_L$ was evaluated by measuring the liquid layer depth $h_L$ and by making use of equations (1) and (2), linking the geometrical quantities shown in Figure 2. Similarly, the interfacial area concentration in its 2D cross-sectional definition can be very easily calculated as the ratio between the length of the chord representing the interface and the cross-section area of the duct.
Uncertainties of the main quantities are reported in Table 2. Further details about repeatability and uncertainty analysis for the same setup and similar flow conditions can be found in [10].

$$\varepsilon_L = \frac{\Omega_L}{\Omega} = \frac{\gamma - \sin\gamma}{2\pi} \text{ (1) and } \gamma = 2\cos^{-1}\left(1 - \frac{2h_L}{D}\right) \text{ (2)}$$

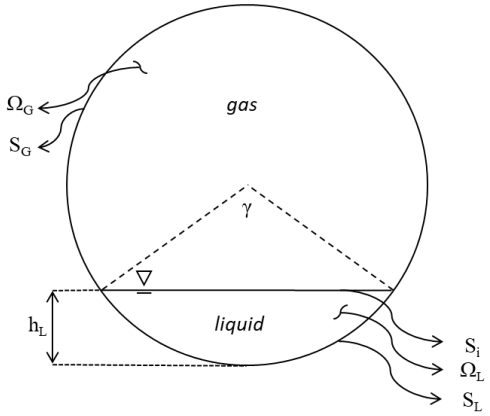


**Figure 2.** Sketch of the phase distribution in the pipe cross section

**Table 2.** Relative uncertainties of the main quantities

| Quantity | $J_G$ [m/s] | $J_L$ [m/s] | $\varepsilon_L$ [–] |
|---|---|---|---|
| Uncertainty [%] | 2 ÷ 7 | 2 ÷ 3 | 1 ÷ 6 |

As anticipated in the Introduction, to measure the liquid height the use of a resistive probe and an image-based, non-intrusive, methods were compared.

Concerning the resistive probe, it is a single-tip, external-electrode resistive probe that consists of the sensing needle, fully insulated apart from the tip, and introduced radially from above into the flow, and of a second wire, submerged into the liquid phase, that acts as a reference electrode. The latter is connected to a +5 V power supply, while the needle is connected to an analogue input of the acquisition board and grounded through a resistor. Since air is not electrically conductive, such a probe allows to sample the state density function (at a frequency of 10 kHz): the voltage signal is zero until the needle touches the liquid phase, then the circuit closes and the signal jumps to a positive value. As the probe is inserted into the duct by means of a probe support endowed with a ruler to provide the immersion depth, when the probe tip touches the liquid the height of the latter can be easily determined. Further details can be found in [10].

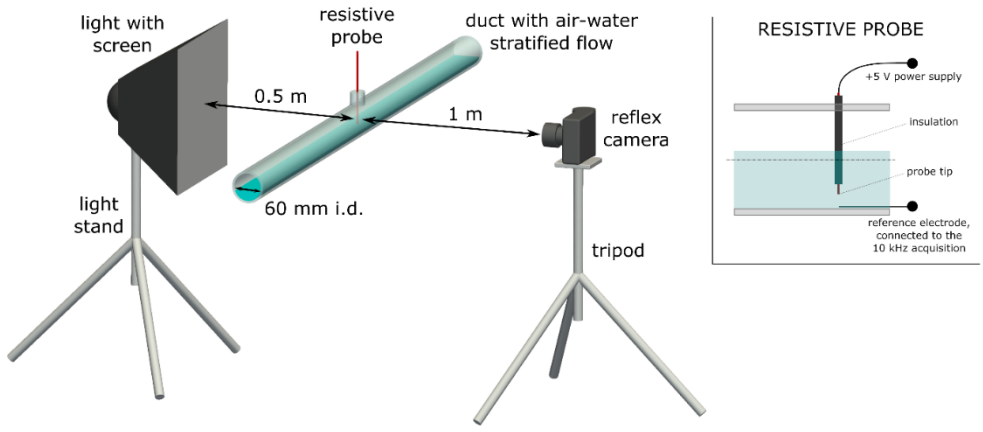


**Figure 3.** Scheme of the experimental setup for the image acquisition, including the duct with an air-water stratified flow, the reflex camera on its tripod and the light with the screen, on its light stand. The resistive probe is also shown in red and sketched in further details in the inset.

As for the image-based measurement, the experimental photographs were acquired using a conventional back-illumination technique, using a photography lamp (800 W) with a diffusing screen and a Nikon D90 single-lens reflex camera with an AF-S Micro NIKKOR 60mm lens. The camera

was placed at 1 m distance from the portion of the pipeline under analysis, whereas the light with the screen was placed at 0.50 m distance from the latter. Both were aligned at the same height of the duct axis. Figure 3 shows a scheme of the experimental setup for the image acquisitions and of the resistive probe. The acquired images were analysed to determine the liquid height by direct measurement of the pixel distance between the duct bottom generatrix and the air-water interface. The interface position is manually identified, as the image characteristics and in some cases the interface waviness make the application of automated interface detection techniques impossible. The duct external diameter is known and provides the pixel-to-meter conversion factor. The liquid height, the liquid holdup and the interface area can be then calculated. As the camera was vertically aligned with the duct axis, while the liquid height was always lower than the latter, due to perspective a small difference between the interface heights in the front and back parts of the duct is present in all the acquired images. Therefore, liquid height was measured at both the front and back triple lines, and the two values were averaged. For each of the images, measurement was also performed in three axial positions, again averaging the results, and by different operators. The latter proved to have a negligible influence on the results.

## 3. Validation of the image-based technique

In the use of the proposed image-based technique, many aspects may in theory originate trueness issues. First of all, the capillary effects, leading to water rise with formation of a meniscus at the duct wall, and the optical distortions due to the changes in refraction indices between water, PMMA and air. Then, in decreasing order of likely importance, also the potential effects of lighting (adequate and in proper position/orientation), field of view and depth-of-field, lens distortion, and sensor resolution should be considered.

Concerning the optical distortion, a preliminary analysis was performed in Matlab® [12] considering 1D optical paths according to the Snell law, as shown in Figure 4, where a ray is traced from an ideal pinhole camera (on the left) to the duct. The real liquid level is drawn in cyan. For better visibility in scheme, the camera in this example is placed at only 0.1 m from the duct axis and the liquid height is set at 10 mm, so the discrepancy between real and apparent levels is much larger than in real experimental conditions. The real results evidenced that given the relatively small thickness of the duct, the distance of the camera from the duct itself and the liquid heights in the investigated flow conditions, the correction is by far lower than the overall experimental uncertainty. As for the capillary effects, Figure 5 shows the shape of the interface and the meniscus for different liquid levels. The interface shape was obtained by CFD simulations of the system, using the Volume-of-Fluid approach in a finite volume framework, by means of the *interFoam* solver of OpenFOAM® [13].

The settings for such simulations are the same as those described in [14]. A value of the water-air surface tension equal to 72 mN/m and a contact angle between water, air and PMMA equal to 70° were considered. These are likely to be not fully accurate values for the investigated flows, so the results should be considered mainly as qualitative ones. Nonetheless, it can be seen how the combined effect of the contact angle and of the inclination of the duct wall with respect to the viewing direction reduces very much the meniscus apparent height for the liquid levels of interest. With the additional consideration that the liquid height is manually identified by the operator, it is possible to conclude that the meniscus is not an issue for the measurement.

As no-truly “reference” technique is available for measurement in this field, validation of the proposed image processing approach was made by using computer-generated images.

Virtual ducts with stratified and stratified-wavy air-water flows were created by the already cited numerical simulations and by the 3D modelling software Art of Illusion [15], exported in Wavefront OBJ format (a format widely used for computer graphics) and rendered with the physically-based rendering engine Appleseed [16]. Duct dimensions (diameter, thickness, etc.) and the camera and light positions with respect to the duct were set to replicate the experimental ones. PMMA and water refractive indices were set to 1.51 and 1.33, respectively. Photorealism in a strict sense was not of interest, the aim was to obtain images including the major optical features of the experimental ones. Figure 6 and Figure 7 show two examples of rendered images compared with the corresponding

experimental photographs of flows with the same liquid height, for a case with a practically flat interface and for a stratified-wavy flow pattern. A small drop, floating on the air-water surface, was also included. Similar drops were occasionally observed in the experimental photographs, and they help in identifying the correct level of the air-water interface.

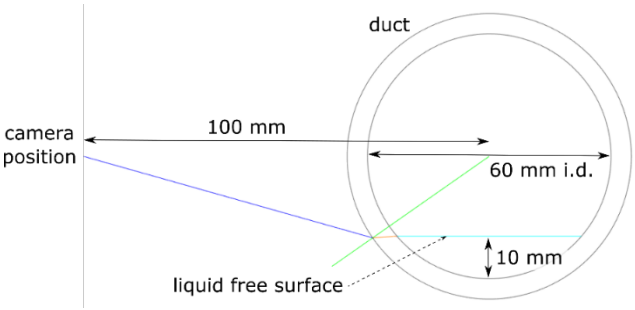


**Figure 4.** An example of the optical ray deviation analysis.

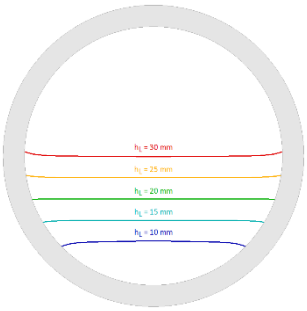

**Figure 5.** Menisci formed by the air-water interface.

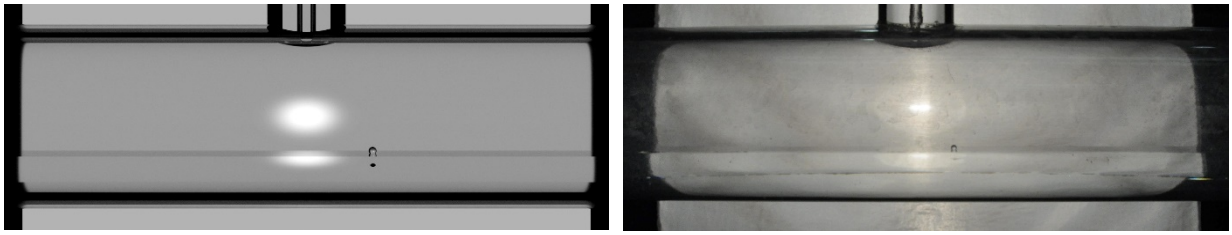

**Figure 6.** An example of rendered flow image (on the left) compared with an experimental photograph of flow with the same liquid height (on the right), for a flow with a practically flat interface

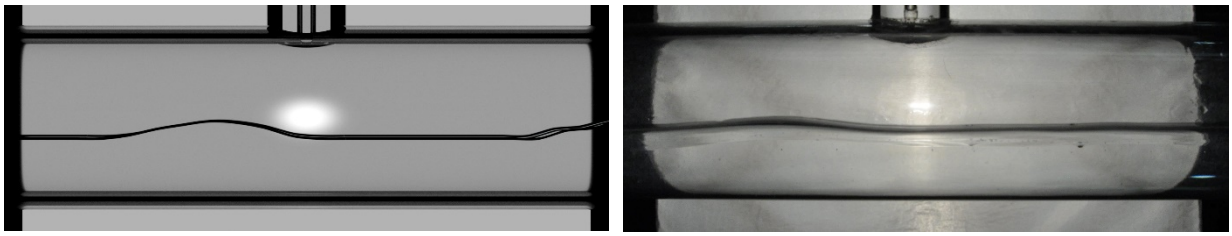

**Figure 7.** An example of rendered flow image (on the left) compared with an experimental photograph of flow with the same liquid height (on the right), for flows with a wavy interface

Measurement of the liquid height on the rendered images was carried out with the same procedure used on the experimental pictures. In each picture, liquid height was measured at both the front and back triple lines, and the two values were averaged. As the liquid was modelled/simulated, its exact height was known, and the measurement error could be calculated. Table 3 reports the results for the investigated liquid heights, both when considering the camera perfectly aligned with the duct and when intentionally introducing a misalignment, to assess the sensitivity of the measure to this parameter. The percentage error shown in the table is calculated as (measured value – true value) / true value · 100. As it can be seen, there are regularities in the errors, as it was expected being the optical paths influenced by the changes in the refraction indices in a deterministic way (they are less affected when the interface is near to the duct mid-plane). A couple of odd values are present, since for those condition the interface was more difficult to identify, and a single pixel of variation significantly changes the error for the rendered images. In any case, the error is always very small, independently from the eventual camera misalignment, and particularly in the range of liquid heights (> 16 mm) of interest for this work.

The vertical shift of the camera with respect to the duct axis that may occur in the experimental campaign is very small, as confirmed by the very thin stripe representing the interface in the experimental photographs. In any case, vertical shifts up to 30 mm – which is an exceedingly large value equal to one half of the duct internal diameter – were investigated, but as they are always very small with respect to the camera distance from the duct (1 m), they have practically no influence on the results. As already said, the measurement is obviously sensitive to errors in the manual selection of the interface, but the high resolution of the experimental pictures (the duct diameter occupies around 830 px, with respect to 260 px in the rendered images) effectively mitigates this issue.

**Table 3.** Results of the measurements on the rendered images

| $h_L$ [mm] | Camera vertical position | Percentage Error [-] |
|---|---|---|
| 11 | aligned with the duct axis | -0.83 |
| 11 | 10 mm higher than the duct axis | -0.83 |
| 11 | 30 mm higher than the duct axis | 0.38 |
| 16 | aligned with the duct axis | -0.33 |
| 16 | 20 mm higher than the duct axis | -0.33 |
| 18.5 | aligned with the duct axis | -0.18 |
| 21 | aligned with the duct axis | -0.07 |
| 21 | 5 mm higher than the duct axis | -0.07 |
| 21 | 30 mm higher than the duct axis | -0.07 |
| 23.5 | aligned with the duct axis | 0.58 |
| 27 | aligned with the duct axis | 0.31 |
| 30 | aligned with the duct axis | 0.00 |

Based on the rendered images, a correction function could also be obtained to account for the effects of the duct curvature and change in the refractive index along the optical path between the interface and the camera. Given the very small values of the errors that can be obtained without any correction, this step would change the final values of the phase fractions by a negligible amount (fractions of percent), so it can be safely skipped in the measurement. In summary, the validation on rendered images proved that the image-based measurement technique can return accurate values of the liquid height.

## 4. Results

Figure 8 shows some representative examples of the acquired images, at the different values of the liquid superficial velocity $J_L$ and gas superficial velocity $J_G$. It can be seen how the liquid height (and therefore the liquid holdup and the interfacial area concentration) increase when both the liquid and the gas superficial velocities are increased. The flow pattern is always stratified, even if small waves appear at the highest superficial velocities. Figure 9 reports the liquid holdup measured with image processing technique, with respect to the liquid holdup obtained using the classical resistive probe method. The values obtained are included in the ± 15 % band, showing a good match for the lower values of the liquid holdup, whereas a worse accuracy is envisaged at the higher liquid holdup values. This is likely due to the presence of small waves in the latter cases. In fact, the liquid height with the image-based method is measured averaging the samples at three different axial coordinates, so it returns a value related to the mean liquid height. On the contrary, with the resistive probe it is assumed that the liquid region has been stably entered when the signal is dominantly zero, so the measured liquid height is nearer to the wave bottom. This results in a lower value of the estimated liquid holdup with respect to the image processing method.

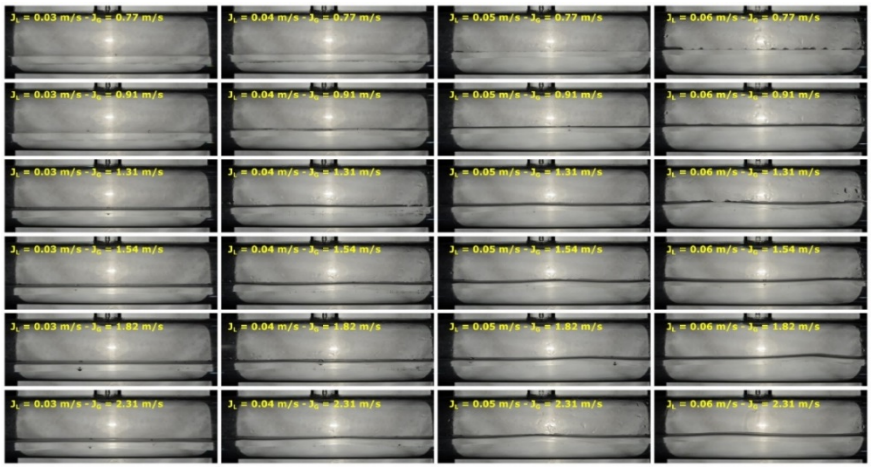

**Figure 8.** Examples of the acquired flow images, at the different values of $J_L$ and $J_G$.

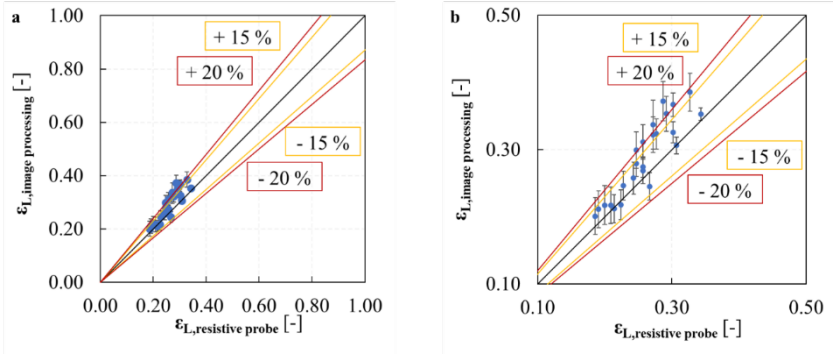


**Figure 9.** (a) Parity plot of liquid holdup obtained through image processing vs. liquid holdup obtained with resistive probe and (b) focus on the region of interest

The obtained results were also compared to three well-known models available in the open literature, the Armand [17], Toshiba [18] and Lockhart-Martinelli [19] models (Figure 10 (a)). Also, in this case the results well agree with the correlations, showing a variation included in ± 15 %, which is an acceptable range for multiphase flows. Whereas in Figure 10 (b) is reported the interfacial area concentration for the various superficial velocities.

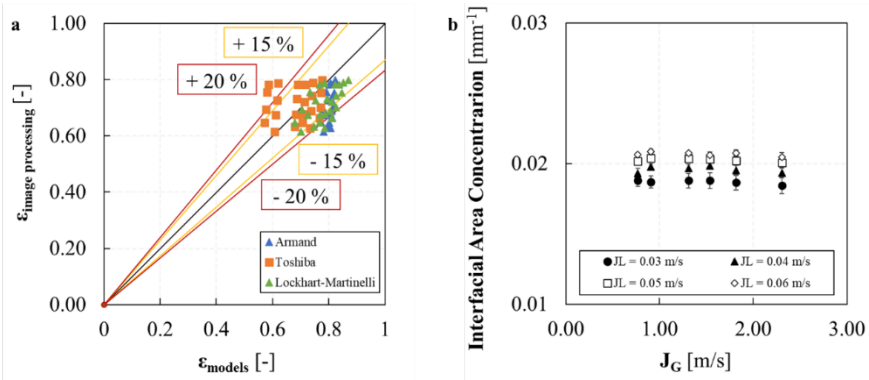


**Figure 10.** (a) Parity plot of gas holdup obtained through image processing vs. gas holdup obtained through models and (b) Interface area concentration vs. Superficial gas velocity

## 5. Conclusions

An image-based technique was tested for the measurement of the liquid height, liquid holdup and interfacial area concentration in stratified flow conditions. The technique was validated on images created by computer graphics and then used on 24 flow conditions at different values of the liquid and gas superficial velocities. The results were compared with those obtained with resistive probes. A very good agreement was found both between the two measurement methods and with the predictions of some widely used literature correlations.

## References

[1] M. Ishii and T. Hibiki, *Thermo-fluid dynamics of two-phase flow*. Springer Science & Business Media, 2010.
[2] M. Guilizzoni, "Flow pattern identification in gas-liquid flows by means of phase density imaging," *Int. J. Multiph. Flow*, vol. 51, pp. 1–10, 2013.
[3] O. C. Jones Jr and J. M. Delhaye, "Transient and statistical measurement techniques for two-phase flows: a critical review," *Int. J. Multiph. Flow*, vol. 3, no. 2, pp. 89–116, 1976.
[4] G. F. Hewitt, "Measurement of two phase flow parameters," *STIA*, vol. 79, p. 47262, 1978.
[5] S. Banerjee and R. T. Lahey, "Advances in two-phase flow instrumentation," in *Advances in nuclear science and technology*, Springer, 1981, pp. 227–414.
[6] N. P. Cheremisinoff, "Instrumentation for complex fluid flows," *CRC Press*, 1986.
[7] O. C. Jones, J. T. Lin, and L. Ovacik, "Investigation of electrical impedance imaging relative to two-phase, gas-liquid flows," *Chem. Eng. Commun.*, vol. 118, no. 1, pp. 299–325, 1992.
[8] S. L. Ceccio and D. L. George, "A review of electrical impedance techniques for the measurement of multiphase flows," *J. Fluids Eng.*, vol. 118, no. 2, pp. 391–399, 1996.
[9] M. Guilizzoni, B. Baccini, G. Sotgia, and L. P. M. Colombo, "Image-based analysis of intermittent three-phase flow," *Int. J. Multiph. Flow*, vol. 107, pp. 256–262, 2018.
[10] I. M. Carraretto, L. P. M. Colombo, D. Fasani, M. Guilizzoni, and A. Lucchini, "Pressure drop and void fraction in horizontal air-water stratified flows with smooth interface at atmospheric pressure," *Fluids*, vol. 5, no. 3, 2020.
[11] L. P. M. Colombo, I. M. Carraretto, A. G. Di Lullo, C. Passucci, and A. Allegrucci, "Experimental study of aqueous foam generation and transport in a horizontal pipe for deliquification purposes," *Exp. Therm. Fluid Sci.*, vol. 98, pp. 369–380, 2018.
[12] "MATLAB." [Online]. Available: www.mathworks.com.
[13] "OpenFOAM." [Online]. Available: https://openfoam.org.
[14] M. Guilizzoni, G. Salvi, G. Sotgia, and L. P. M. Colombo, "Numerical simulation of oil-water two-phase flow in a horizontal duct with a Venturi flow meter," *J. Phys. Conf. Ser.*, vol. 1224, no. 1, 2019.
[15] "Art of Illusion." [Online]. Available: http://www.artofillusion.org.
[16] "Appleseed." [Online]. Available: https://appleseedhq.net.
[17] A. A. Armand, "The resistance during the movement of a two-phase system in horizontal pipes," *Izv Vse Tepl Inst. 1*, pp. 16–23, 1946.
[18] P. Coddington and R. Macian, "A study of the performance of void fraction correlations used in the context of drift-flux two-phase flow models," *Nucl. Eng. Des.*, vol. 215, pp. 199–216, 2002.
[19] R. W. Lockhart and R. C. Martinelli, "Proposed correlation of data for isothermal two-phase, two component flow in pipes," *Chem. Eng. Progr.*, vol. 45, pp. 39–48, 1949.